

# Land cover change estimation in Brazil through direct photointerpretation and supervised classification, a case study

**David Lopez Cornelio<sup>†</sup>**

Faculty of Life and Environmental Sciences, Shimane University, Japan

E-Mail: davlzo@hotmail.com | Fax: 4734669

## **Abstract**

A representative area of Manaus (Brazil) was evaluated from Landsat TM images taken two years apart. A method is proposed to reliably discriminate major classes of land cover in remote areas, employing a neural networks-based classification, cloud masking, and noise reduction filters for image enhancement. The results showed the dispersion of located areas of forest recovery at an average rate of 0.3% and forest degradation at an average rate of 0.65% annually. A main factor is the distance to human settlements and ways of transportation. Unexpectedly, these effects are likely to be accelerated the more distant they are from major cities. This confirms the complexity of the causes, tendencies and variability in time and space of deforestation. The method proved to be reliable for cases in which because of inaccessibility, ground truth data cannot be obtained.

Keyword : land cover change detection, tropical deforestation, remote sensing, supervised classification.

## **Introduction**

Land cover is defined as the observed physical cover, as seen on the ground or through remote sensing, including vegetation and human constructions, which cover the earth's surface (LUCC, 2000). In recent years, much attention has been focused on tropical forests. As much as 50% of their original extent has been lost to deforestation in the last two decades, primarily as a result of agricultural expansion. Global estimates of tropical deforestation range from 69,000 km<sup>2</sup>/year in 1980 to 165,000 km<sup>2</sup> in the late 1980s (Table 1); 50 to 70% of the more recent estimates have been produced in the Brazilian Amazon, the largest continuous region of tropical forest in the world (WRI, 1990).

Our understanding of tropical deforestation is inadequate for two reasons: lack of accurate measurements of the rate, geographic extent and spatial pattern of

deforestation, and lack of insight regarding its causes. Tropical deforestation is the consequence of a variety of interrelated social, economic, and environmental factors, yet interpretations of how these factors influence deforestation vary widely. Some focus chiefly on population growth, while others regard institutions as the main determinant.

Table 1. Extent of today's rain forests in the world and rate of deforestation. Vandermeer and Perfecto (1995).

Region	Current extent (millions km <sup>2</sup> )	Annual deforestation (millions km <sup>2</sup> )
America	4	0.19
Asia	2	0.22
Africa	1.8	0.05
Africa	1.8	0.05

Satellite observations provide an objective and quantitative approach to the measurement of land cover change, the conversion from active agriculture to secondary forest (regrowth), the spatial geometry of land cover change, and the patterns of land use by type in the long term considering past and present trends. A number of techniques for detection of change have been formulated, applied and evaluated. These techniques can be grouped into two general classes: (1) those based on spectral categorization (classification) of the input data; and (2) those based on radiance change between acquisition dates. Within the first type are procedures that (a) assess change based on categorization and subsequent comparison of the results from each date; or (b) assess change based on direct two-date categorization. Procedures within the second classification include (a) band subtraction, (b) transformed band subtraction, (c) rationing, (d) regression, (e) principal components and (f) multi-spectral change vector magnitude and direction. Hybrid approaches based on a mix of categorical and radiometric change information have also been proposed and evaluated.

Among the factors governing selection of a change detection strategy are information requirements, spectral coverage, data availability and quality, image processing resources, analyst skill and experience, phenomenological knowledge, time and cost constraints, and the importance of labeling the changes that are detected. (Johnson and Kasischke, 1998). Although Jeanjan and Achard (1997) found a consistent relationship between deforested areas measured at fine spatial resolution and fragmented forest proportions mapped at coarse spatial resolution, Borak et al. (2000) noted that different resolutions can measure different land cover change processes. In their study of an area in the Amazon, Mausel et al. (1993) were able to accurately classify (82–88%) three classes of secondary succession forests (initial,

intermediate and advanced) using Thematic Mapper (TM) images. The age of regenerating tropical forests can also be approximated through time-series of Landsat and SPOT sensor data (Lucas et al, 2002). Changes in spectral reflectance (explained in terms of temporal changes in canopy geometry and leaf area) can be summarized by indices related to canopy brightness and greenness (Steininger, 1996). Although Maximum Likelihood classification confuses much of the recently burned forest with non-forest classes, and is unable to classify older burned forests (Cochrane and Souza, 1998), texture-based classification using TM data and post-classification by fuzzy classification output accurately mapped regenerating tropical forest classes in a region in Amazonas (Palubinskas et al, 1995). The present study estimates the rates and patterns of major land cover change processes over two years in a representative area of the Brazilian Amazon region.

### **Study area**

The study area is located at 3° 13' S latitude and 60° W longitude (path 231 and row 062). Since the early 1970s, the Brazilian government introduced ambitious road building and colonization programs intended to develop the region. Together with generous fiscal incentives, these policies set in motion movement of ranchers, miners and small-plot farmers into the region (Skole and Justice1, 1997). The climax ecosystem is the lowland rain forest. The upper stratum (35–45m) of this formation is composed of a few evergreen or briefly deciduous species, well distributed in age. The age distribution of the upper layer is irregular and the canopy, observed from high above, appears very irregular and undulating. Swamp forests are present along the rivers. These formations are influenced by the presence of frequent floods and soils with poor drainage. The upper canopy layer (up to 45m in some cases), composed of a small number of species, is quite homogeneous compared to the lowland rain forest.

Where extended flooding and poor drainage conditions preclude the subsistence of trees, large swamps grasslands appear in the forest domain, usually at the periphery of swamp forests. Corridors of secondary forest formations are along the old road network. A complex of secondary regrowth, fallow, home gardens, and food crops form the vegetation found here. Boundary between forest types is sometimes very fuzzy and, in the case of visual interpretations, different interpreters can assign pixels differently (Mayaux et al, 2002). Distinction between the permanently and periodically flooded forests could not be achieved in thematic maps derived from optical remote sensing data.

Table 2 Land cover classes in the Manaus region (Steininger, 1996).

**Pasture:** Grassland for cattle grazing with no standing trees or large areas of bare soil.  
**Pasture with trees:** Grassland for cattle grazing with standing live trees.  
**Agriculture:** Mostly manioc, sometimes inter-cropped with vegetables.  
**Regrowth:** Even-aged stands of unmanaged secondary regrowth in fallowed or abandoned lands previously used for pasture or agriculture.  
**Mature forest:** In terra firme, lands with no known recent disturbance due to clearing or logging.

Deforestation was slow until the early 1980s, Landsat MSS imagery acquired in 1982, revealed that many large cattle pastures had been or were in the process of being formed. By 1985, the area deforested for pasture had not expanded greatly, although several areas of previously untouched forest had been cleared for use as commercial plantations (e.g. oil palm). In 1991, Landsat TM imagery revealed that much of the land cleared for agricultural use had degraded and was in a state of regeneration (Lucas et al, 2002). The study area exemplifies roadside forest conversion to small and medium-sized pasture and agriculture, and includes numerous stands of forest regenerating from pastureland abandonment in the early 1980s (Table 2). The land use patterns of the area are typical of much of the tropical forest clearance and abandonment throughout Amazonia (Steininger, 1996). Early regrowth has a very dense shrub forest canopy three to four meters high, which is composed mainly of primary succession species (mostly *Cecropia* spp.). Regrowth up to eight years maintains an even overstory canopy, and a dense understory of secondary succession species develops. Older regrowth (10 to 20 years) has a less even canopy and begins to approach mature forest in stature. In this area the “dry” season extends from June to September and the “humid” season from October to May (Fig. 2). Biomass vigor, cloudiness and periodical floodings in the area are directly related to precipitation and temperature (Fig. 2). In the image from August 1998 the low density of foliage crops made the identification of the regrowth class easier and burned areas were also expected. In the image from May 2000 (b2000) the percentage of cloudiness was over 30%.

## **Methodology**

Two full scenes 6100 pixels by 5760 lines in size and covering an area of approximately 183 km by 172 km were compared. They are composed of six bands, and are referenced to the UTM coordinate system. Three samples were located along the Pan American Highway, north of Manaus city and the Amazon river (Fig. 1). The image processing and analysis (Fig. 3) were carried out according to the following sequence:

- 1) Spectral patterns determination: by displaying in graphs the behavior of each band in 3x3 pixel plots taken from b1998 image for each class. The pixels considered were those situated at the center and corners of each subsample. The digital numbers per band follow almost the same trend, with slight differences in bands 4, 5 and 7.

Regrowth and Forest classes have similar digital numbers, typically lower than the Non Forest class (Fig. 4). The greater the distance between numbers in the feature space distribution, the greater the potential for accurate between-class discrimination. As noted above, the spectral patterns of the Regrowth and Forest classes are similar. Band 5 and to some extent bands 4 (Forest class) and 7 (Non Forest class) give better differentiation of spectral reflectance from adjacent pixels. Although some speckled misclassification of Forest as Regrowth is expected due largely to local terrain effects (Steininger, 1996), the latter class has lower reflectances in the infrared.

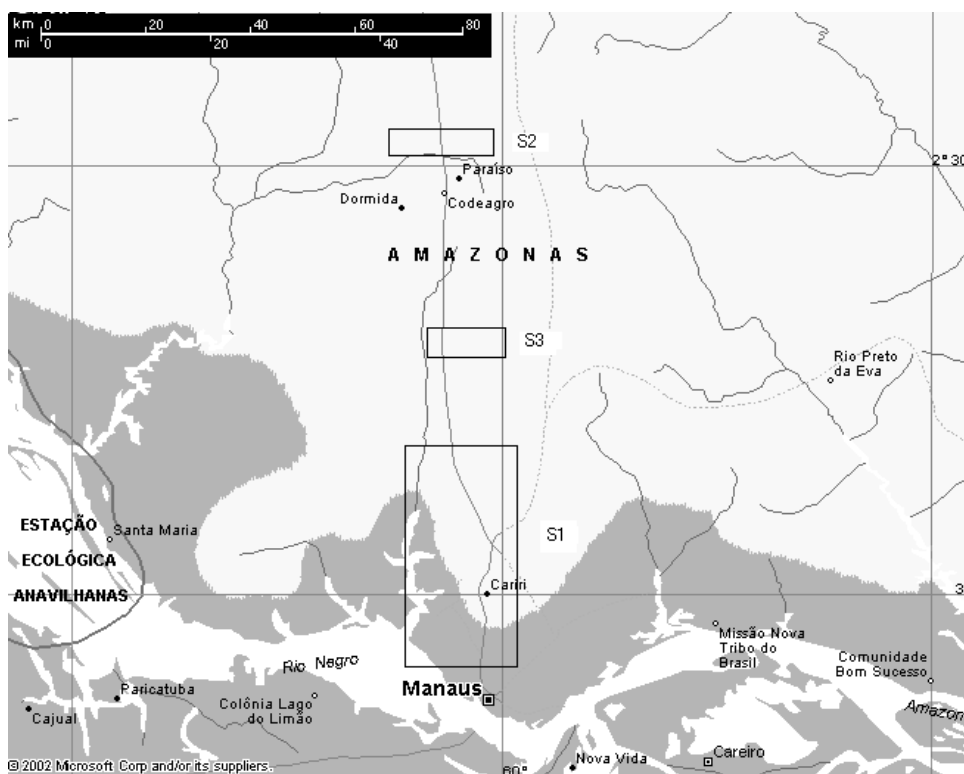


**Fig. 1.** Location map of the study areas. Source: [www.expedia.com](http://www.expedia.com)

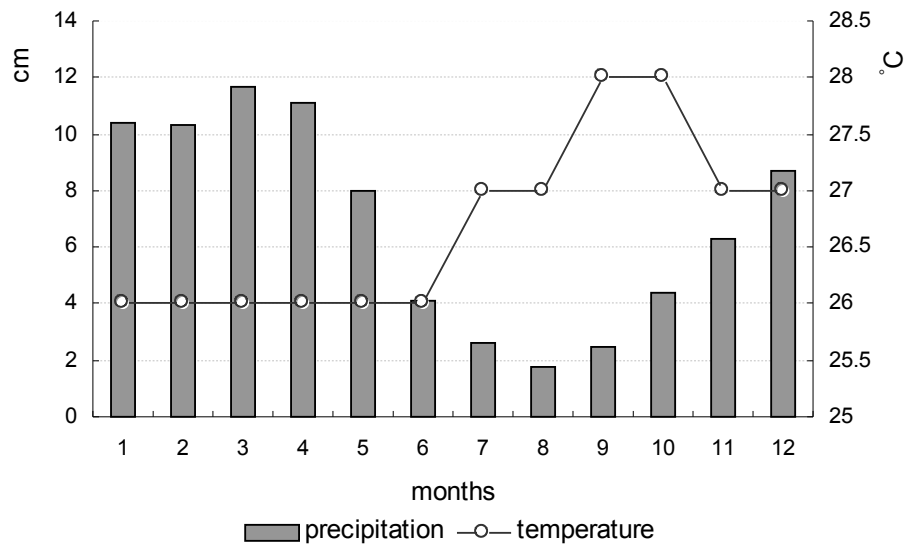


**Fig. 2.** Weather conditions (Manaus, 1998).

Source: [www.curriculumvisions.com/weather](http://www.curriculumvisions.com/weather)

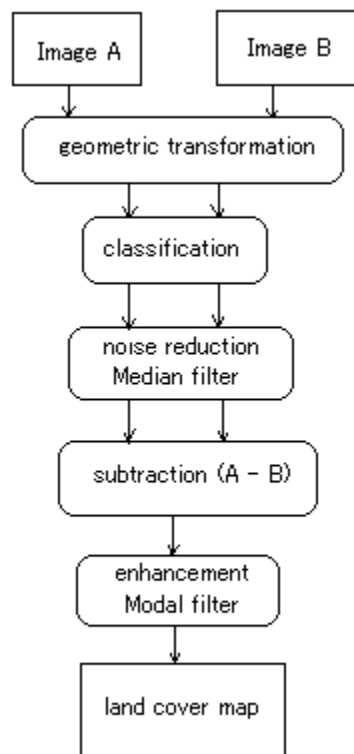


**Fig. 3.** Procedure flowchart

**Table 3** Location and geometrical characteristics of the study sites (subareas).

SUBAREA	I	II	III
Perimeter (km)	146.0024	113.9406	102.9433
X extent (km)	26.5682	45.5299	30.3646
Y extent (km)	46.439	11.4404	21.1071
Area (km <sup>2</sup> )	1233.6401	520.879	640.907
Lines	1554	385	704
Columns	883	1521	1012
Center Latitude	S 2 50' 12"	S 2 12' 49"	S 2 28' 56"
Center Longitude	W 60 05' 41"	W 59 58' 30"	W 59 59' 19"

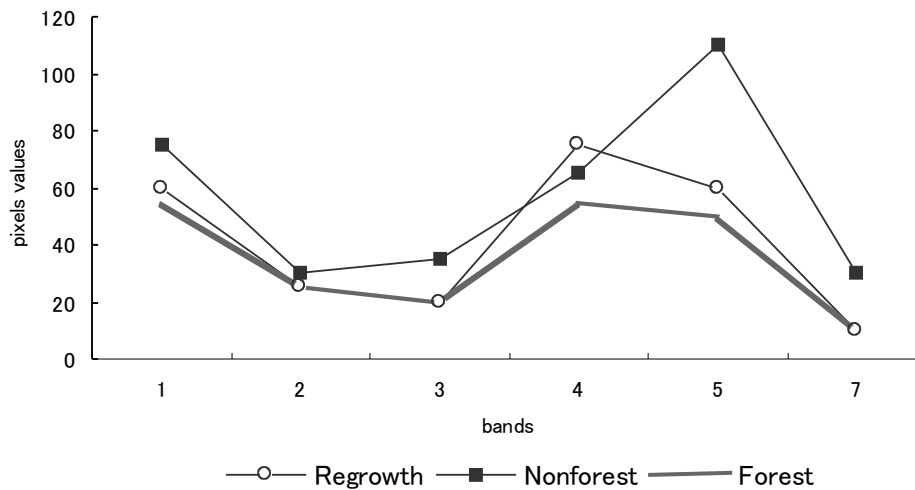


**Fig. 4.** Mean signature values for three selected land cover types across bands 1, 2, 3, 4, 5 and 7.

2) Radiometric and geometric rectification: Radiometric correction for sensor and atmospheric effects was performed first because in the raw data there is direct relation between the scan line of each sensor and its position in the sensor array; after the geometric correction this relationship is altered or lost. The histogram matching technique using the cumulative histograms of two sensors (b2000 having b1998 as reference) was used for the radiometric correction. To permit classification of both images using the same training data set they were resampled by cubic interpolation. Geometric transformation enables repositioning of pixels within an image (Table 3), and can be used to register multiple images and restore geometric distortion caused by lens aberration and viewing geometry (Baxes, 1994). Cubic Interpolation, rather than assuming linear relations between two known cell values,

determines a new cell value by fitting the cubic polynomial surface to a 4x4 array of cells. This generally produces a very smooth output raster object (Microimages, 2002). Experience recommends using this method with continuous data types where cell values represent scalar quantities such as elevation or temperature. However, here performed better than the nearest neighbor method which is suitable for discrete input cell data such as soil types or crop categories. This last method produced discontinuities and lower overall accuracy, because some input values may be used more than once as output values, whereas other input values may not be used at all (Ilwis, 2002). Results of this operation are shown in Table 4.

Table 4 Pixel characteristics after geometric transformation

	Cell size (m)		Central point		DN (band 3)		Raster	
	Column	Line	Latitude	Longitude	Mean	Std.Dev.	Min.	Max.
Before	29.9972	29.9975	S 20°50'12"	W 60°005' 41"	19.0139	3.9617	13	155
After	29.9972	29.9975	S 20°29'00"	W 59°059' 04"	19.017	3.7274	11	143

3) Subareas extraction and classification: a reference map built on a red green-blue display (RGB) with 3-2-1 bands (normal color) was used for construction of the training data. Another display with 7-5-4 bands (best spectral separability) was used to calculate the accuracy of classification. The classes listed in Table 2 were grouped into three: Forest class (mature forest), Non Forest class (agriculture, pasture and pasture with trees) and Regrowth class. Bodies of water were not included in the results since they are considered as unchangeable area. Since field data were not available, the training data were identified by tone, texture and location, using the Steininger (1996) land cover map of the area as a reference. The subareas were classified using a Stepwise Linear supervised classifier.

The characteristics of the subareas are described in table 3. The three samples were located near Manaus and along Route 174 (Fig 1 and Table 4). Land cover change is spatially concentrated, so accurate determination of change is difficult to achieve by a “random sampling” analysis of digital data, unless a very high percentage of the area to be studied is sampled (Tucker and Townsend, 2000). Construction of the training data set using the Feature Map option of TNTmips software, and the classification results are shown in figure 5 and table 5 respectively. The Feature mapping process provides computer-assisted classification for images otherwise

suiting only for direct photointerpretation by drawing or painting features over the reference image. A training set or prototype is a group of sample cells in an image known to represent a feature type or ground cover of interest (Microimages, 2002). To be mathematically correct (Ilwis, 2002), half of the ground truth data was used for the sample set and the other half for the test set. Size per class is shown in table 5. We assumed that “degradation” (dim gray, white or dim green) was concentrated around human settlements, roads and rivers, diminishing in intensity until becoming forest (dark green). Clouds were masked during the classification. The method employs a statistical technique that calculates a set of derived variables (discriminant functions), which produce the best possible discrimination between the classes in the training data set (Microimages, 2002). The selected classifier, the stepwise linear discriminant analysis, determines decision rules that enable the classification of desired features. The greater overall accuracy and cleaner resultant map than with parametric classifiers are explained by a strong correlation between output values for a given class and the proportions of that class for all test regions combined (Frizzelle and Moody, 2001). The overall accuracy for the class Forest was 99.32%, for the Non Forest class 59.24%, for the Regrowth class 98.92% and for the Water class 98.75%. The overall accuracy was calculated by dividing the total number of correctly classified raster cells by the total number of cells in the ground truth raster, and expressing the result as a percentage. Since the standard Kappa index of agreement is usually not appropriate (Pontius, 2000) it was not considered for the assessment of accuracy.

Values on the diagonal of the Normalized Co occurrence Matrix have the same class number on the horizontal and vertical axis, and thus measure the spatial properties of the individual classes (Table 6). Negative values indicate that the cells in the class tend not to be adjacent to each other, and that the class is thus diffusely fragmented into many small areas.

**Table 5** Training data set and resultant cells per class after classification.

	Training Set		b1998		b2000		DIF.
	Cells	%	Cells	%	Cells	%	%
<b>Subarea 1</b>							
Forest	22327	68.9169	1095738	80.81	1063554	79.58	-1.23
NonForest	3315	10.2324	106416	7.85	113416	8.49	0.64
Regrowth	490	1.5125	103865	7.66	111609	8.35	0.69
<b>Subarea 2</b>							
Forest	21338	81.1025	443173	85.61	429284	84.56	-1.05
NonForest	4083	15.504	42143	8.14	45839	9.03	0.89
Regrowth	914	3.4707	32319	6.24	32551	6.41	0.17
<b>Subarea 3</b>							
Forest	17532	74.544	604766	89.85	622261	90.36	0.51
NonForest	3875	16.476	26866	3.99	25860	3.76	-0.23
Regrowth	2112	8.98	41440	6.16	40497	5.88	-0.28

4) Image enhancement: Noise reduction and enhancement were achieved by applying 3x3 median and modal filters respectively. To eliminate noise, the classified maps for the three samples were enhanced through a Median Filter 3x3, to remove non-random noise, thin lines and isolated points. The 5x5 kernel eliminates such noise entirely but also loses detail. This filter weights each cell in the kernel equally and computes a median for the cell being processed. A Modal 3x3 filter was then applied for the land cover change rasters (subtraction b2000-b1998) to smooth detail and remove noise. This also weights each cell in the kernel the same and computes the mode for the cell being processed.

5) Comparison of classified images, and visualization of areas of change in binary maps. The pixel value of the classified raster (4bit unsigned) for Forest class (dark green) was 1; for Non Forest (yellow) was 2 and for Regrowth (clear green) was 5. The raster obtained after subtraction ( $C=A-B$ ) was 8 bit unsigned, where areas that remained as Non Forest class are in white, and those that remain as Regrowth class are gray. Zero values denote areas of no change, and positive and negative values (reclassified as 1) denote areas of change (Lo and Shipman, 1990). The resultant map recognizes Regrowth and Non Forest areas that reconverted to Forest within 21 months, or, Regrowth areas that converted to Non Forest. Roads and rivers provide access to loggers, cultivators and encroachers who can cause deforestation (Fig. 6a and 6b). They also connect farmers to urban markets, promoting cash crop cultivation if transport costs are attractive. Roads are still few and far between over large areas of the humid tropics (Apan and Peterson, 1998), so rivers often remain the chief means of communication and permanent cultivation tends to be concentrated close to waterways

Table 6 Normalized Co occurrence Matrix

	b1998			b2000		
	Forest	NonFore	Regrow	Forest	NonFore	Regrow
Subarea 1						
Forest	-0.395			-0.378		
NonForest	-0.173	-0.463		-0.18	-0.231	
Regrowth	-0.176	-0.067	-0.298	-0.177	-0.259	-0.337
Subarea 2						
Forest	-0.494			-0.466		
Non Forest	-0.169	0.087		-0.174	0.366	
Regrowth	-0.153	1.071	1.19	-0.123	0.899	0.497
Subarea 3						
Forest	-0.678			-0.708		
Non Forest	-0.108	0.905		-0.117	2.129	
Regrowth	-0.15	-0.504	0.89	-0.146	1.559	1.119

**Fig. 5.** Class change in 21 months. (a) raw image displayed in natural colors, (b) training data set on 7-5-4 RGB display of bands, (c) classified map (filtering and masking were applied), (d) vector layer overlaid on the result of {classified map 2000 – classified map 1998}, the areas that changed are shown in white, roads in red, Non Forest areas in yellow and Regrowth areas in green. The background map was enhanced with a Modal 3x3 Filter.

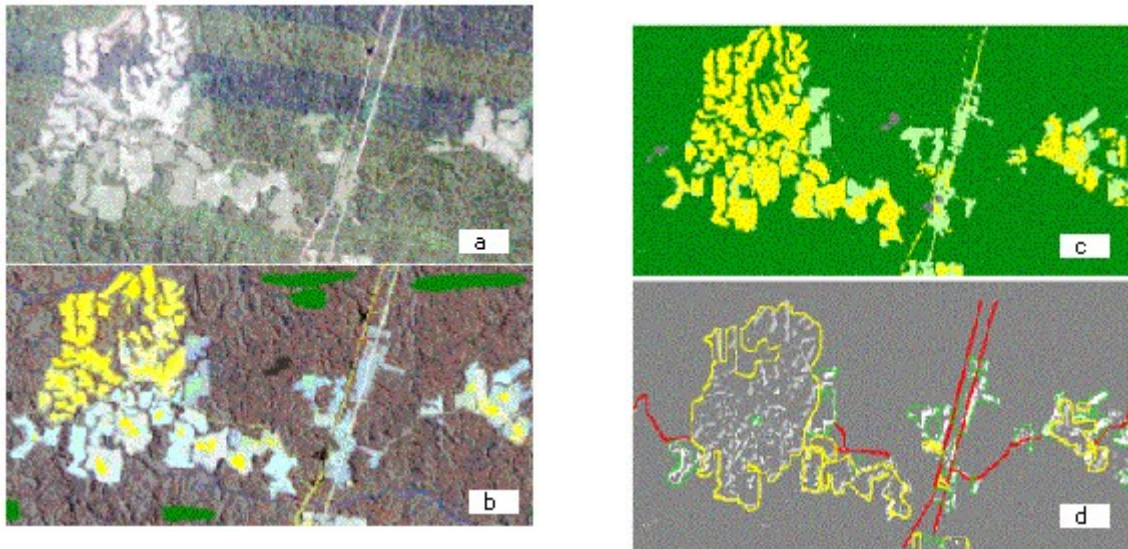


**Fig. 6a.** Change along road. 40x40 pixels section ( $1.428 \text{ km}^2$ ) from subarea I.

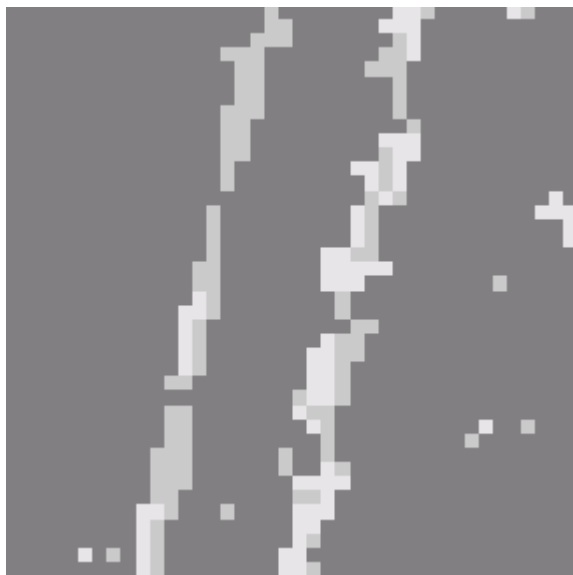


**Fig. 6b.** Change along river. 40x40 pixels section ( $1.428 \text{ km}^2$ ) from subarea II

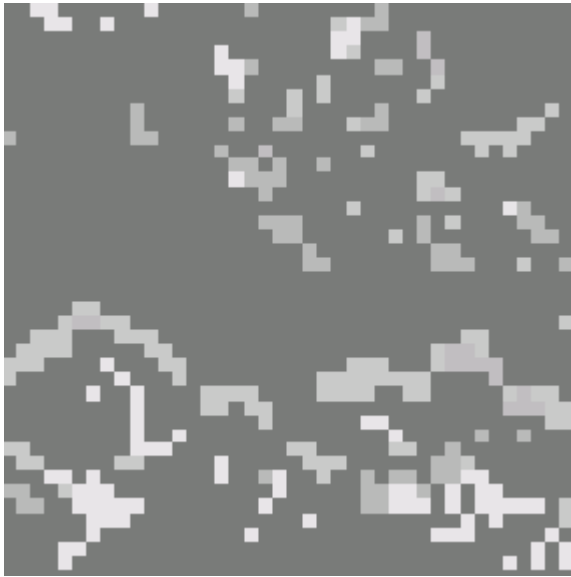
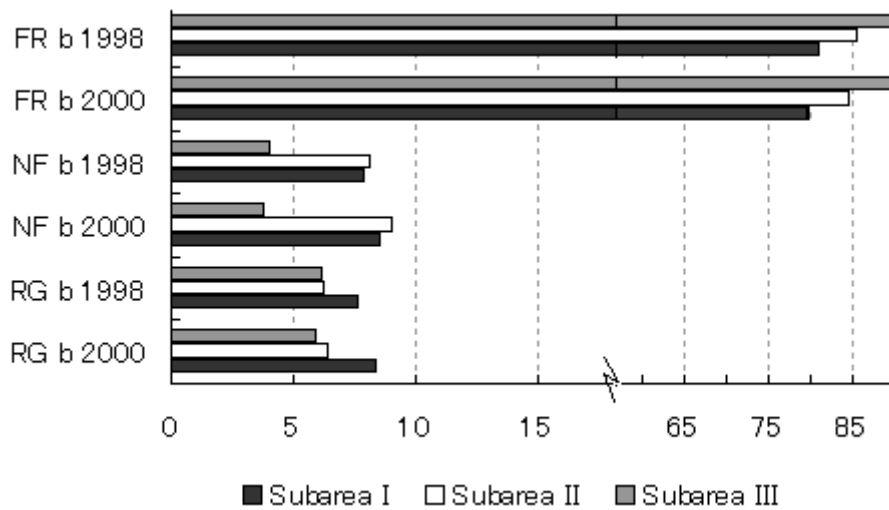


**Fig. 7** Change in Forest (FR), Non Forest (NF) and Regrowth (RG) classes in percentage for the three Sub areas, in 1998 and 2000 year.



**Results and discussion**

Over 21 months, the Regrowth class increased in subareas I (0.69%) and II (0.17%) but decreased in subarea 3 (-0.28%) (Fig. 7). The Non Forest class increased in

subareas I (0.64%) and II (0.89%) but decreased in subarea III (-0.23%) (Fig. 8). The Forest class decreased in size in subareas I (-1.23%) and II (-1.05%) but increased in subarea III (0.51%) (Fig. 9). The Forest class area in subarea I declined 1.23% at the expense of an almost equal increment in Non Forest (0.64%) and Regrowth (0.69%) areas (Table 5). The Forest class area also decreased 1.05% In subarea II at the expense mainly due to an increment in the Non Forest class areas of 0.89%, slight increment (0.17%) also occurred in the Regrowth class. In subarea III the Forest class increased 0.51% while the Non Forest and Regrowth classes decreased almost uniformly (-0.23% and -0.28% respectively). Skole and Justice2 (1997) highlighted the important role of secondary growth (regrowth) in the overall dynamics of deforestation, where the rate of abandonment is often as high as the rate of deforestation but lags by 5–8 years. Regrowth may be large and growing, while deforestation rates are declining. The values on the diagonal of the Normalized Co-occurrence Matrix (Table 6) have the same class number on the horizontal and vertical axis, and thus measure the spatial properties of the individual classes. Greater rates of change are explained by diffused fragmentation of the class into many small areas; slow rates are associated with the occurrence of relatively large, homogeneous areas. In subarea I, negative values indicate that the cells in the class tend not to be adjacent to each other, and that the class is thus diffusely fragmented into many small areas. In subarea II, the Forest class is also diffusely fragmented into many small areas. The Non Forest class has a random distribution, occurring in areas of random size and purity. The Regrowth class in b1998 occurs in relatively large, homogeneous areas (many cells of the same class lie adjacent to each other), whereas in b2000 it displays a random spatial distribution, occurring in areas of random size and distribution. In subarea III, the Forest class is diffusely fragmented into many small areas; the Non Forest and the Regrowth classes occur in relatively large, homogeneous areas, particularly in b2000 (Table 6). Further studies are needed to understand the causes of land cover class aggregation/desegregation after colonization. It is well known that during the early stages of colonization, smallholders establish tenure claims by clearing land along any border of their property that is likely to be challenged. After roads are opened, an initial row of farms with fronts of several hundred meters facing the road is rapidly established. As these sites closer to the road are taken, second, third and more parallel rows of farms are established, each a couple of kilometers inside the forest (Sierra, 2000). Agricultural expansion reduces the amount of natural fuel standing in the landscape. Consequently increased of landscape fragmentation may cause reduction in the spontaneous propagation of fires, although forest fragmentation caused by selective logging may be an important exception (Eva and Lambin, 2000). The rates of secondary growth (regrowth or forest regeneration) can be as high as those of deforestation in some areas, and is commonly distributed around the Non Forest class areas. This could be one cause of reported overestimation of deforestation by over 50% (Skole and Tucker, 1993; Hudak and Wessman, 2000). It is also possible

that, as in the case Cross River State in Nigeria (Ite and Adams, 1998), the actual process of forest loss at the local (village) level can be slow and gradual, while being considered high at the level of broad aggregate national data. Farms with a similar percentage of forests and cover composition are more likely to have higher rates of deforestation the more distant they are from the major cities (subareas II and III). This corroborates what McCracken et al. (1999) found in a study of regression analysis on patterns of deforestation/forestation in the state of Para (Brazil). They found coefficients associated with distance indicated a curvilinear relationship between distance and annual area deforested. Further interpretation of sequential multitemporal data would confirm these results. On the grounds that deforestation can change dramatically from one year to the next (Skole and Justice1, 1997), average annual estimates over several years may miss important events, such as years in which the rates are significantly higher or lower than in other years.

### **Conclusions**

Forest degradation was detected at a rate ranging from 1.05 – 1.2 %, mainly because of an 0.6–0.9% increase in Non Forest areas and secondarily, due to increase in Regrowth areas (0.2 – 0.7%). Also, in some areas decrease in Non Forest and Regrowth areas reflects an increase in Forest areas by 0.5% over 21 months. This study shows that it is possible in this region to detect land cover changes in the main classes with accuracy when ground survey is unavailable. With maps of previous studies as reference, training data can be successfully built on a “natural color” display. Secondary growth (forest regeneration) in Amazonia is a dynamic vegetation class in the forested–agriculture interface, and the rates of forest recovery can be greater than that expected. If estimates of the areas and rates of land abandonment can be made with similar accuracy of deforestation estimates, this alone can provide valuable information about the fate of cleared tropical forests.

### **Acknowledgements**

My thanks to Dr. Barry Roser for comments on the manuscript. Financial support for this study was provided by the Ministry of Education of Japan.

## References

- Apan A. and Peterson, J. 1998. Probing tropical deforestation—the use of GIS and statistical analysis of georeferenced data, *Applied Geography* 18(2): 137–152.
- Baxes, G. 1994. *Digital image processing: Principles and applications*. 480pp, John Wiley and Sons, New York, 69–122.
- Borak, J., Lambin, E. and Strahler, A. 2000. The use of temporal metrics for land cover change detection at coarse spatial scales. *Int. J. Remote Sens.* 21: 1415–1432.
- Cochrane, M. and Souza, C. 1988. Linear mixture model classification of burned forests in the Eastern Forests. *Int. J. Remote Sens.* 19: 3433– 3440.
- Eva, H. and Lambin, H. 2000. Fires and land–cover change in the tropics: a remote sensing analysis at the landscape scale, *Journal of Biogeography* 27(3):765–767.
- Frizzelle, B. and Moody, A. 2001. Mapping continuous distributions of land cover: a comparison of maximum–likelihood estimation and artificial neural networks, *Photogrammetric Engineering and Remote Sensing* 67(5): 693–705.
- Hudak, A. and Wessman, C. 2000. Deforestation in Mwanza District, Malawi, from 1981 to 1992, as determined from Landsat MSS imagery, *Applied Geography* 20(2): 155–175.
- Ilwis. 2002. Online GIS software tutorial, retrieved from [www.itc.nl/ilwis](http://www.itc.nl/ilwis).
- Ite, U. and Adams, W. 1998. Forest conversion, conservation and forestry in Cross River State, Nigeria, *Applied Geography* 18(4): 301–314.
- Jeanjean, H. and Achard, F. 1997. A new approach for tropical forest area monitoring using multiple spatial resolution satellite sensor imagery. *Int. J. Remote Sens.* 18: 2455–2461.
- Johnson, R. and Kasischke, E. 1998. Change vector analysis: a technique for the multispectral monitoring of land cover and condition. *Int. J. Remote Sens.* 19: 411–416.
- Lo, C. and Shipman, R. 1990. A GIS approach to land use change dynamics detection, *Int. J. Remote Sens.* 56(11): 1483–1491.

Lucas, R., Honzak, M., Amaral, I., Curran, P. and Foody, G. 2002. Forest regeneration on abandoned clearances in central Amazonia, *Int. J. Remote Sens.* 5: 965–988.

LUCC. 2000. Meeting in the middle: the challenge of meso-level integration, an international workshop, LUCC report serie 5, October 17–20, Ispra, Italy.

Mausel, P., Wu, Y., Li, Y., Moran, E., and Brondizio, E. 1993. Spectral identification of successional stages following deforestation in the Amazon, *Geocarto International* 4:61–71.

Mayaux, P., de grand, G., Rauste, Y., Simard, M. and Saatchi, S., 2002, Large-scale vegetation maps derived from the combined L-band GRFM and C-band CAMP wide area mosaics of Central Africa, *Int. Remote Sensing*, 2002, 23(7), 1261–1282.

Mc Cracken, D., Brondizio, E., Nelson, D, Moran, E. and Siqueira, A. and Rodriguez-Pedraza C. 1999. Remote sensing and GIS at farm property level: demography and deforestation in the Brazilian Amazon, in *Photogrammetric Engineering and Remote Sensing*, 65 (11): 1311–1320.

Microimages. 2002. Online reference manual, retrieved from: [www.microimages.com](http://www.microimages.com)

Palubinkas, G., Lucas, R., Foody, G., and Curran, P. 1995. An evaluation of fuzzy and texture-based classification approaches for mapping regenerating tropical forest classes from the Landsat TM data. *Int. J. Remote Sens.* 16, 747–759.

Pontius, R. 2000. Quantification error versus location error in comparison of categorical maps, *Photogrammetric Engineering and Remote Sensing*, 66 (8): 1011–1016.

Sierra, R. 2000. Dynamics and patterns of deforestation in the western Amazon: the Napo deforestation front, 1986–1996, *Applied Geography* 20(1): 1–16.

Skole <sup>1</sup>, D. and Justice, C. 1997. A land cover change monitoring program: A federal agency initiative. Retrieved 1/25,2/25,5/25 from <http://www.bsrsi.msu.edu/overview/reports/cenr.html>

Skole <sup>2</sup>, D. and Justice, C. 1997. Acquisition and analysis of large quantities of data for measuring land cover change, retrieved 3/18, 5/18,4/18 from <http://www.bsrsi.msu.edu/overview/landsat7ft.htm>

Skole, D., and Tucker, C. 1993. Tropical deforestation and habitat fragmentation in the Amazon: Satellite data from 1978 to 1988. *Science* 260: 1905-09.

Steininger, M.. 1996. Tropical secondary forest regrowth in the amazon: age, area and change estimation with Thematic Mapper data. *Int. J. Remote Sens.* 17: 9-27.

Tucker, C. and Townshend, R. 2000. Strategies for monitoring tropical deforestation using satellite data. *Int. J. Remote Sens.*21:1461-1471.

Vandermeer, J. and Perfecto, I. 1995. Breakfast of biodiversity, the truth about rain forest destruction, the Institute for Food and Development Policy, Oakland, California, USA, 183pp.

Wilkie, D. and Finn J. 1996. Remote sensing imagery for natural resources monitoring, a guide for first time users, Columbia University Press, 295 pp.

WRI. 1990. World Resources 1990-1991. Oxford Univ. Press, New York.